Nanostructure criteria for lithium intercalation in non-doped and phosphorus-doped hard carbons

Herbert H. Schönfelder, Kenshin Kitoh, Hiroshi Nemoto

NGK Insulators, Ltd., Corporate Research and Development Group, 2-56 Suda-Cho, Mizuho-Ku, Nagoya 467, Japan

Abstract

Hard carbons from various precursors heat-treated at 1000–2000 °C follow a common rule with regard to their structure–capacity correlation for lithium intercalation. A nanostructure containing a large fraction of highly strained carbon layers with large interlayer spacings and small crystallite sizes is a prerequisite to achieve reversible capacities in the range 300–450 mAh/g. P-doping of carbon derived from a polymer precursor causes a softening of the hard carbon structure by decreasing the strain on carbon layers, reducing interlayer spacing and increasing the crystallite sizes. It also induces a reduction of the number of nanopores which become larger in size. The amount of space reduction by the softening effect, however, is more than compensated by the dopant so that capacities of 550 mAh/g and first cycle efficiencies improved up to 83% are achieved. © 1997 Published by Elsevier Science S.A.

1. Introduction

Carbon materials as the anode for lithium-ion batteries proved to be the most effective hosts for lithium in rechargeable lithium batteries. Carbons are superior to alternative materials in terms of safety, cycleability and long-term stability. Recently, certain hard carbons synthesized at temperatures just above the dehydrogenation temperature (1000 °C) have attracted attention due to their high reversible lithium intercalation capacity at moderate capacity losses during the first charge/discharge cycle [1].

In this study it is demonstrated that a specific set of carbon structure parameters is critical for reversibly accommodating a significant amount of lithium ions. Furthermore, the strong effect of dopants on that nanostructure, leading to an improvement of reversible capacity as well as first cycle efficiency, is shown.

2. Experimental

Two sets of carbons were prepared from different precursors. The first set contained non-doped carbons made from phenol resin (A), epoxy resin (B), and three commercial carbons (C), (D), and (E) heated to 1000 °C. (A) and (B) were pyrolyzed under argon atmosphere at heating rates of 5–10 K/min to end temperatures of 1000, 1200, 1400, 1600 and 2000 °C.

The second set consisted of P-doped carbons derived from epoxy resin which was dissolved in an organic solvent to which phthallic anhydride hardener and phosphoric acid were added. The acid content was varied to 5, 9, 19 and 38 wt.% of resin. The clear solution was dried to remove the solvent and hardened at 120 °C for 14 h. The product was then heated under argon atmosphere at heating rates of 5–10 K/min to end temperatures of 900, 1000, 1100, and 1200 °C. The phosphorus content was determined by inductively coupled plasma (ICP) analysis, the oxygen content by gas chromatography. The type of bonding partners within the carbon material and their bonding energies were determined by X-ray photoelectron spectroscopy (XPS) with C(1s), P(2p) and O(1s) measurements.

The structure parameters were determined by rotary target powder X-ray diffraction (XRD) and subsequent computerized calculation of a fitting curve using a structure refinement program for disordered carbons [2]. Although P-doped carbons in part contain a significant amount of phosphorus, the program was also applied to these samples in order to obtain a first-order structural information. Small-angle X-ray scattering (SAXS) data were collected at 2θ from 0.8 to 10° in transmission mode with a sample thickness of 1.5 mm and polyimide windows. The disorder structure was also inves-

tigated by laser Raman spectroscopy with an argon-ion laser beam of 50 mW power. Transmission electron micrographs (TEM) were taken from selected samples to confirm the structural data. Pyrolyzed and ground carbon powder was investigated along the thin powder grain margins in order to avoid any structural modification by conventional TEM sample thinning techniques. Specific surface areas were determined by standard BET method.

The electrochemical cells consisted of carbon powder mixed with polyvinylidene fluoride (PVDF) binder and printed on copper plates as a current collector, a porous polymer separator, a lithium metal counter electrode and a liquid electrolyte containing $LiClO_4/EC + DEC$. Cells were cycled at 25 mA/g between 0.002 and 1.5 V.

3. Results and discussion

The structural parameters and capacities of a variety of non-doped carbons are shown in Fig. 1. The typical bimodal character of the nanostructure is detected by the structure parameter g which is calculated from the (002) peak in XRD by a strain probability distribution function [2]. At low temperatures, samples A–D revealed high values of $1 - g$ which represented the calculated volume fraction of highly strained, non-parallel layers of carbon. $1 - g$ decreased with temperature as the structure rearranges towards more parallel layer-

Fig. 1. Structure parameters and capacity vs. heat-treatment temperature of non-doped hard carbons.

ing. The following two parameters described the structure in the low strain regions g. The lateral crystallite size L_a was in the 16–18 Å range for the samples A–D at 1000 °C and increased in a linear way with temperature. Simultaneously, the interlayer spacing d_{002} from which the line broadening effect of the average spacing fluctuation δ was subtracted, decreased. The reversible capacity of samples A–D with high values for $1 - g$ and d_{002} as well as small L_a was in the range 300–450 mAh/g. In contrast, the comparative sample E showed low $1 - g$ and d_{002} in combination with larger L_a resulting in a lower capacity of 230 mAh/g at 1000 °C.

Although these parameters are not independent from each other, they help to visualize the preferred structure type. The parameters point to a spacious nanostructure being able to accommodate a large amount of lithium. For hard carbons, it is essential to inherit this structure from their precursors directly after carbonization as an increase in temperature does not produce such structures any more. At 2000 °C, the structures of all samples are similar and their capacities low.

Analysis of TEM confirm the bimodal nanostructure of hard carbons. Regions of parallel layering can be distinguished from spacious areas with random layer orientation. Furthermore, the presence of nanopores for sample B is detected by SAXS. The average radius of gyration of the pores is 5.5 Å at 1000 °C. There is less than one order of magnitude difference between the small size of the nanopores and the interlayer spacing d_{002}. Hence, the pores can be regarded as an extreme case of lattice disorder and may be the result of more pronounced random layer orientation.

The addition and homogeneous distribution of a dopant such as phosphoric acid within the carbon precursor has a strong effect on the carbon structure. In Table 1 are shown: the structure parameters; the chemical compositions; the size of nanopores and the electrochemical properties of carbons derived from epoxy resin at different doping levels and temperatures (see also Fig. 2). At 1000 °C the high strain regions $1 - g$ reduce in volume from 0.74 to 0.55 and L_a increases from 17 to 21 Å for the samples with 0 and 19% acid addition (0 and 10 wt.% P), respectively. Notably at the same time, the average pore size almost doubles from 5.5 to 9.3 Å (Fig. 2). If we consider the nanopores to be an extreme case of lattice disorder, this indicates an order/disorder polarization of the bimodal nanostructure as compared with non-doped samples. The regions with more parallel layering occupy a larger volume fraction while the nanopores become larger in size. At the same time the intensity of the small angle X-ray scattering spectra decrease which implies a reduction in pore number and volume thus providing the space needed to accommodate the larger crystallites. Specific surface areas of several powdered samples are in the range of 1.5–2.4 m²/g. This shows that the nanopores cannot be accessed by the nitrogen gas used in standard BET method. This may be due to the fact that the nanopores are closed or that their entrances are smaller than the nitrogen molecules.

Parallel layering, increase in L_a and reduction of d_{002} are clear signs of the softening of the hard carbon structure which
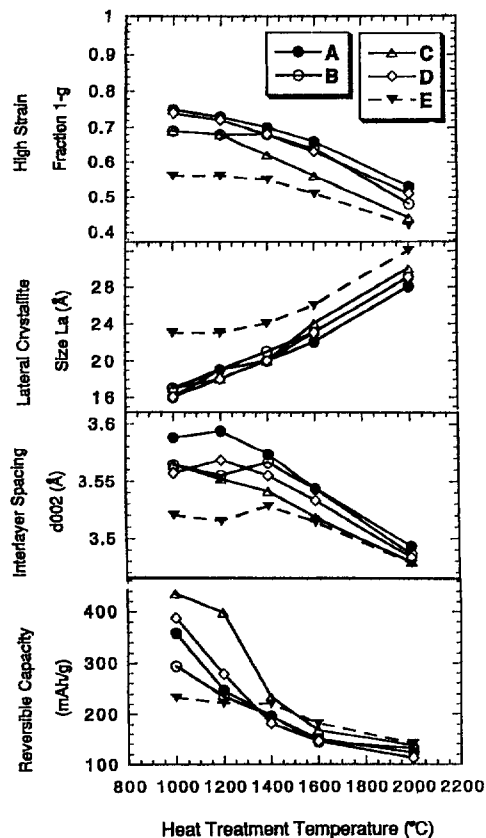
Table 1
Summary of chemical, structural and electrochemical data of P-doped carbons prepared from epoxy resin

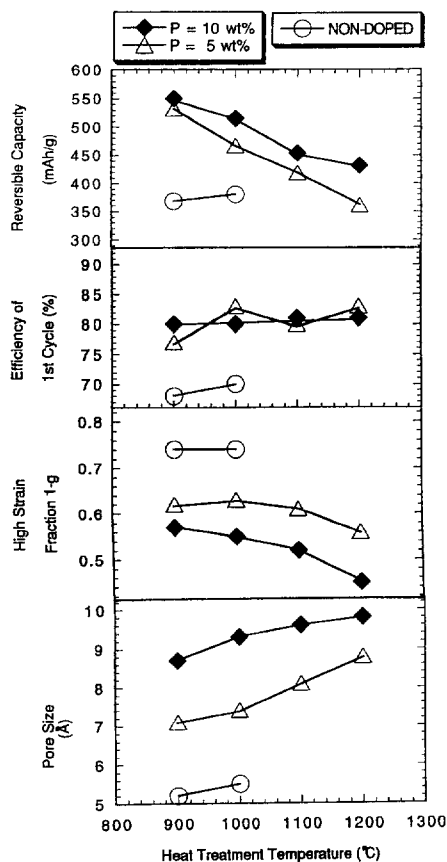| Acid addition (wt.% of resin)	Heat-treatment temperature (°C)	P-content of carbon (wt.%)	O-content of carbon (wt.%)	High strain fraction, $1-g$	Interlayer spacing, $d_{(002)}$ (Å)	Lateral crystallite size, L_a (Å)	Pore size, R_g (Å)	Reversible capacity (mAh/g)	First cycle coulombic efficiency (%)
0	900			0.74	3.585	16	5.2	368	68
5	900	2.84	2.87	0.71	3.551	16	6.1	415	68
9	900	5.28	1.08	0.62	3.536	17	7.1	532	77
19	900	9.89	1.18	0.57	3.505	19	8.7	550	80
38	900	13.9	4.95	0.64	3.488	21	10.3	540	70
0	1000			0.74	3.593	17	5.5	380	70
5	1000	2.90	1.35	0.68	3.565	18	6.3	424	66
9	1000	5.17	0.49	0.63	3.536	18	7.4	467	83
19	1000	9.61	0.64	0.55	3.516	21	9.3	515	80
38	1000	13.30	7.21	0.56	3.493	23	10.0	530	78
9	1100	5.20	0.35	0.61	3.541	20	8.1	419	80
19	1100	9.47	0.64	0.52	3.511	23	9.6	454	81
38	1100	10.26	1.24	0.51	3.489	26	10.3	464	78
9	1200	4.99	0.25	0.56	3.529	22	8.8	361	83
19	1200	9.38	0.66	0.45	3.498	25	9.8	432	81
38	1200	8.97	0.90	0.46	3.482	26	10.8	417	75

Fig. 2. Capacity, efficiency, high-strain fraction, and pore size of P-doped hard carbon.

may be caused by the dopant. In order to understand this mechanism the presence of phosphorus within the structure will be investigated.

XPS analysis exhibits that the phosphorus is largely bonded directly to carbon by covalent bonding and does not intercalate between the layers or form a secondary phase derived from the $(PO_4)^{3-}$ ions of the phosphoric acid. Merely within a fine surface layer on the carbon/air interface phosphorus is oxidized. This layer has no detrimental effect on the initial charge/discharge process. The presence of P–C bonds is a result of an effective bonding reaction between the polymer precursor and phosphoric acid on a molecular scale in solution. Based on calculation we can estimate that in a carbon with 10 wt.% P, on average, one phosphorus atom is surrounded by 25 carbon atoms.

Laser Raman spectra show clear peak shifts between the non-doped and P-doped samples (Table 2). At 1000 °C, P-doping causes an upshift of both E and D peaks by 10–20 cm^{-1}. According to calculations on model carbon structures containing both $(sp)^2$- and $(sp)^3$-type carbon bonds conducted by Beeman et al. [3], an increase in $(sp)^3$-type bonding results in a downshift of both E and D peaks. Inversely, we can infer that an upshift of both peaks indicates a reduction of the $(sp)^3$ bonds. As the three-dimensional $(sp)^3$-bonding between carbon layers in hard carbons may be one reason for the fact that it is non-graphitizing the elimination of such

bonds by phosphorus is an explanation for the softening effect of P-doping on the hard carbon structure detected by XRD. Furthermore, this would imply that phosphorus is most likely coordinated by only three carbon atoms in a planar configuration similar to the $(sp)^2$-type carbon–carbon configuration in order to allow parallel layering assuming that phosphorus is equally distributed between low and high strain regions. Finally, the slight decrease in I_D/I_E peak intensity ratio also gives evidence of improved order.

Comparison of the voltage curve for de-intercalation of lithium between non-doped and P-doped carbons reveals that the latter has a de-intercalation plateau in the 700–1100 mV range. This leads to an extension of reversible capacity for lithium. Although the amount of reversible capacity that can be reached below 500 mV is smaller for the doped samples, the large extent of the plateau at higher voltage level yields a total capacity that is far larger than that of the non-doped sample. Thus the effect of reduced structural space can be more than compensated by the dopant. The intercalation and de-intercalation plots of voltage versus capacity are similar to those reported for hydrogen-containing carbons [4]. Analogously, we infer a mechanism by which lithium is bonded to phosphorus at a low voltage during intercalation and debonded at a higher voltage during de-intercalation leading to a hysteresis. This corresponds to the mechanism reported for hydrogen-containing carbons, however, the plateau and thus the capacity caused by P-doping is maintained at heat-treatment temperatures of carbon between 900 and 1200 °C at which hydrogen has already largely diffused out of the carbon.

The P-bonding/debonding mechanism is very efficient raising overall charge/discharge coulombic efficiencies to around 80% during the first cycling (Fig. 2). The improved layering of the carbon structure may also contribute to high efficiencies due to lower resistance to lithium-ion diffusion. At further cycles, efficiencies stabilize around 98%, however, total capacities decrease.

Doping levels of 5–10 wt.% P are most effective in terms of improving capacity and efficiency. Lower dopant levels reduce these properties, higher dopant levels (13 wt.% P) reach a saturation point were it becomes difficult to accommodate more phosphorus in the carbon structure by the solution process.

Table 2
Laser Raman data from hard carbons with and without P-doping

Heat-treatment temperature (°C)	P-content (wt %)	Peak shift		Intensity ratio I_D/I_E
		E ($(sp)^2$)	D ($(sp)^3$)	
1000	0	1590	1335	0.8
1000	5 17	1600	1355	0.6
1000	13 30	1600	1355	0.6
1200	4.99	1605	1365	0.6

4. Conclusions

Detailed analysis of the structure variations within the non-doped hard carbons permits the definition of a preferred structure for high lithium capacity based on the volume fraction of high strain $1 - g$, the lateral crystallite size L_a and the interlayer spacing d_{002}. The parameters indicate the necessity for a spacious structure in order to achieve high lithium intercalation capacities.

The carbon precursor with the addition of phosphoric acid yields a carbon material with a polarization of a nanostructure. Both, the volume fraction of low strain g and the size of the nanopores are large. The presence of phosphorus bonded to the carbon layers on a molecular scale has a softening effect on the hard carbon. The carbon layers obtain a more parallel orientation with less interlayer space. However, the amount of space reduction due to the doping process is more than compensated by the P-bonding effect of lithium. Capacities of 550 mAh/g and first cycle efficiencies of up to 83% are achieved.

References

[1] T. Zheng, Q Zhong and J.R. Dahn, *J Electrochem Soc., 142* (1995) 11.
[2] H. Shi, J. Reimers and J.R. Dahn, *J. Appl. Crystallogr., 26*t (1993) 827.
[3] D. Beeman, J Silverman, R. Lynds and M.R. Anderson, *Phys. Rev, B30* (1984) 870.
[4] J.R. Dahn, T. Zheng, Y. Liu and J.S. Xue, *Science, 270* (1995) 590.